Assessing the influence of calibration methodology and model structure on glacio-hydrological simulations in the Cheakamus River Basin, British Columbia, Canada

Kai Tsuruta & Markus A. Schnorbus

2022

Pacific Climate Impacts Consortium (PCIC)

PCIC Publications

Original citation:

Tsuruta, K., & Schnorbus, M. A. (2022). Assessing the influence of calibration methodology and model structure on glacio-hydrological simulations in the Cheakamus River Basin, British Columbia, Canada. *Journal of Hydrology* X, *17*, 100144. https://doi.org/10.1016/j.hydroa.2022.100144

Journal of Hydrology X 17 (2022) 100144

Contents lists available at ScienceDirect

Journal of Hydrology X

journal homepage: www.sciencedirect.com/journal/journal-of-hydrology-x

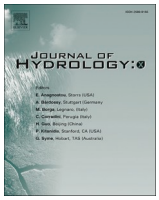

Research papers

Assessing the influence of calibration methodology and model structure on glacio-hydrological simulations in the Cheakamus River Basin, British Columbia, Canada

Kai Tsuruta, Markus A. Schnorbus *

Pacific Climate Impacts Consortium, University of Victoria, Victoria, British Columbia, Canada

ARTICLE INFO

This manuscript was handled by Marco Borga, Editor-in-Chief, with the assistance of Francesco Avanzi, Associate Editor

Keywords:
Glacier dynamics
Glacio-hydrological model
Calibration uncertainty
Hydrological projections

ABSTRACT

As glaciers across the world continue to recede, there is a concern that their loss as a fresh water reservoir within mountainous basins will have a negative impact on stream temperatures and downstream water resources. Currently, there are relatively few glacio-hydrological models (GHMs) appropriate to study such phenomena and studies that have used GHMs generally acknowledge the high uncertainty associated with their simulations. Calibration techniques present a particular issue in GHMs as available glacier observations are limited and errors in the glacierized portion of a basin can be compensated by errors in the non-glacierized portion. Using as a study site the Cheakamus Basin in British Columbia, Canada, we 1) present a new, fully-coupled GHM, 2) analyze the effects different calibration techniques have on the model's summer streamflow projections, and 3) compare the fully-coupled GHM results to projections using a one-way GHM. The calibration techniques studied vary in terms of glacier representation (dynamic/static), and glacier constraint (mass balance/thinning rates/thinning rates and area change). We find projected future climate forcings are sufficiently strong in the Cheakamus Basin so as to generally make the sign and significance of changes to the basin's hydrology insensitive to the calibration and projection procedures studied. However, the variation among these procedures produces significant changes in the projected magnitude of future hydrological changes and therefore should be carefully considered in studies where precision beyond the sign and significance of change is required. Based on analysis of the variation within each procedure's set of model outputs, we conclude 1) the two-way GHM has benefits over the one-way model, 2) calibration using dynamic glaciers and a thinning rate constraint is preferable for the new GHM, and 3) there is a need for additional studies on the uncertainties associated with the calibration of glacio-hydrological models.

1. Introduction

Alpine glaciers worldwide are generally thought to be in a state of recession (Gardner et al., 2013; Kaser et al., 2006) that is expected to continue through the end of the century (Radić and Hock, 2011). From a water resources and environmental perspective, the global impact of this continued glacial loss may be substantial (Barnett et al., 2005; Huss and Hock, 2018). Over one-sixth of the world's population depends on glacier and snowmelt for their water supply (Barnett et al., 2005) and in even modestly glacierized basins (2 −5%glacial coverage), glacier melt has been shown to play a significant role in seasonal streamflow (Stahl and Moore, 2006). Glacial melt usually coincides with the warm, dry weather that is typically associated with low flow periods in the non-glacierized portions of the basin (Meier, 1969) and warm stream temperatures (Brown et al., 2005; Moore, 2006). Hence, in partially glacierized basins, glaciers can compensate for otherwise low flow conditions and act to attenuate stream temperatures and variability in the streamflow signal (Fountain and Tangborn, 1985). As a basin's glacial area decreases, its ability to attenuate stream properties may ultimately diminish. While initially glacier loss is associated with an increase in melt and subsequent streamflow, this benefit is not sustained as the supply of glacier ice is eventually exhausted (Huss et al., 2008; Stahl and Moore, 2006). In those regions dependent on melt from diminishing glaciers, estimating the current and future stages of the basin's streamflow relative to this changing glacier signal is an important task (Frans et al., 2015).

Despite the importance of understanding a region's streamflow response to glacier loss, projecting the future hydrology of partially glacierized watersheds remains a difficult challenge. Amongst other facets, long-term simulations must model how the glacier volume and

* Corresponding author.

https://doi.org/10.1016/j.hydroa.2022.100144
Received 8 April 2022; Received in revised form 24 October 2022; Accepted 10 November 2022
Available online 1 December 2022

area evolve over time. This requirement is juxtaposed with the common practice of hydrological models assuming a static glacier coverage and glacier dynamics models not being linked to other hydrological processes (Naz et al., 2014). While recent studies have developed and deployed coupled glacio-hydrological models (GHMs; e.g, Immerzeel et al. (2012); Ismail et al., 2020; Jost et al., 2012; Naz et al., 2014; Seibert et al., 2018), there are still relatively few models available that use physically based representations to simulate both glacier dynamics and hydrological processes.

Of the studies focused on GHMs, many have raised the issue of the high uncertainty associated with their simulations. For hydrological models in general, uncertainty in the future forcings (Blöschl and Montanari, 2010), the representation of hydrological processes (Orth et al., 2015), and the calibration/validation approach (Troin et al., 2016) all contribute to uncertainty in simulation results. In partially glacierized basins, uncertainty in calibration is exacerbated by relatively limited observations of the processes controlling glacier dynamics (van Tiel et al., 2020) and the possibility that errors in the glacier portion of the basin may compensate for errors in the non-glacierized portion (Ismail et al., 2020). For proper interpretation of projection results from GHMs, the relative magnitude of each source of uncertainty should be understood.

Recently, some progress has been made towards understanding and better constraining the uncertainty in GHMs. Naz et al. (2014) compared the metric performance over a 22-year historical period of streamflow from the distributed hydrology soil-vegetation model when using 1) static glaciers, 2) prescribed glaciers based on observations, and 3) glaciers simulated using a dynamics model. In that study, the authors found that including a glacier dynamics representation improved prediction of streamflow as simulation length increased, and that the hydrographs produced using prescribed and modelled glacier changes were similar over the historic period. In Ismail et al. (2020), the future hydrology in the Upper Indus Basin was projected using two GHMs each parameterized using 1) a "simple" calibration/validation approach that only used streamflow observations at the basin's outlet and 2) an "enhanced" calibration/validation approach that incorporated subcatchment gauge data, different climate conditions, and glacier mass balance. The study found some differences in the projected streamflow between the two methods at the annual scale (up to 10%) as well as larger monthly differences (up to 19%) during colder months (October-March). Using analysis of variance, Ismail et al. (2020) also found that by the end of the century, uncertainty associated with parameterization using the enhanced method was very small relative to overall uncertainty and therefore concluded that an enhanced calibration approach may help constrain hydrological projections. In Tsuruta and Schnorbus (2021), the authors analyzed the variability in projected streamflow from a one-way GHM with prescribed glaciers that stemmed from choice of 1) glacier evolution, 2) parameterization amongst Pareto optimal sets, and 3) climate forcings. The study found the uncertainty associated with choice of climate forcings to be largest and the uncertainty associated with choice of parameterization among Pareto optimal solutions (from the same calibration procedure) to generally be larger than the uncertainty associated with choice of glacier evolution.

While these previous studies have provided useful insights regarding GHM uncertainty, our collective understanding of the impacts of calibration/validation approaches and glacier dynamics representations on GHM uncertainty is still relatively underdeveloped. Recently, van Tiel et al. (2020) performed a thorough review of calibration procedures currently used for GHMs and concluded there is need for a systematic analysis of best practices for GHM calibration to better understand model simulations in glacierized basins.

To this end, we explore the impact that different calibration procedures have on the streamflow changes projected by a fully coupled GHM in the partially glacierized Cheakamus River Basin. For simulations, we use a new GHM that represents the full coupling of the UBC Watershed Model (UBCWM) to the regional glaciation model (Clarke et al., 2015). The three procedures were selected based on available data and the methodology of previous studies (i.e. Ismail et al. (2020); Jost et al., 2012; Lutz et al., 2016; Meyer et al., 2019; Tsuruta and Schnorbus, 2021). All of the procedures use the same optimization algorithms and streamflow targets, but vary in the glacier data used to constrain simulations and the treatment of glacier dynamics during the calibration period (see Fig. 1 and Section 2.4). To compare the fully coupled GHM model structure to our previous work's methodology, we also analyze projections that use the one-way coupled model from Tsuruta and Schnorbus (2021) wherein prescribed changes to glacier landcover based on Clarke et al. (2015) results are forced annually onto UBCWM simulations.

2. Methods

2.1. Study Site

We simulate the hydrological processes of the Cheakamus Basin up to its gauging station approximately 6 km north of its confluence with the Squamish River near the southwestern coast of British Columbia (Fig. 2). The Cheakamus Basin was selected for this study because of the availability of observational glacier and hydrological data, projected glacier dynamics (i.e. Clarke et al. (2015) simulations), and historic and projected forcing data. It was also selected because it is of operational interest. The basin is regulated roughly 24 km upstream of its Squamish River confluence by the Daisy Lake Dam which is operated by BC Hydro. The simulated basin has a drainage area of 965 km^2 with elevation ranging between roughly 2300 m and 50 m. Hydrologically, the basin is considered a hybrid regime. Snowmelt dominates the annual streamflow signal, but is superimposed by short, intense fall and winter rain-on-snow events that typically account for the highest daily flows. The basin is mostly forested ($>$ 60%) with modest glacier coverage ($\sim$ 5%) that is thought to be in a state of recession (Bolch et al., 2010). Only a small portion ($\ll$1%) of the basin is considered urban.

2.2. Models

In our study, we generate projections of the hydrology of the Cheakamus Basin in two ways: 1) With a fully-coupled glacio-hydrological model, and 2) with a one-way coupled glacio-hydrological model. The two approaches vary only in the method used to calculate the change in the glacier coverage. In the fully-coupled approach, the basin's glacier coverage is updated at the end of each water year based on simulations using the regional glaciation model (RGM), which is driven by annual mass balance states of the hydrological model. In the one-way approach, annual glacier coverage is dictated by the results of the simulations described in Clarke et al. (2015) (See Section 2.3 of this paper). In both approaches, we discretize the Cheakamus Basin into 200 m $\times$ 200 m hydrological response units (HRUs). This resolution was chosen to match that of the RGM simulations and Clarke et al. (2015) results, allowing for straightforward interfacing of the hydrological and glacier components of the GHM. We model the hydrology of an individual HRU using the University of British Columbia Watershed Model (UBCWM). Routing within and between subbasins and calculations of streamflow contributions are handled by Raven's internal algorithms. Below, we provide a brief overview of the main components of our modeling framework.

2.2.1. Raven

Raven is a modular hydrological modeling framework described in Craig et al. (2020). In its original design, Raven was capable of applying landuse change only if the changes were known prior to the beginning of the simulation. For our purposes, we modified Raven's source code to allow landuse change to be determined during a simulation based on output from an external program (e.g., RGM). This modification allows one to create within Raven a GHM consisting of any combination of

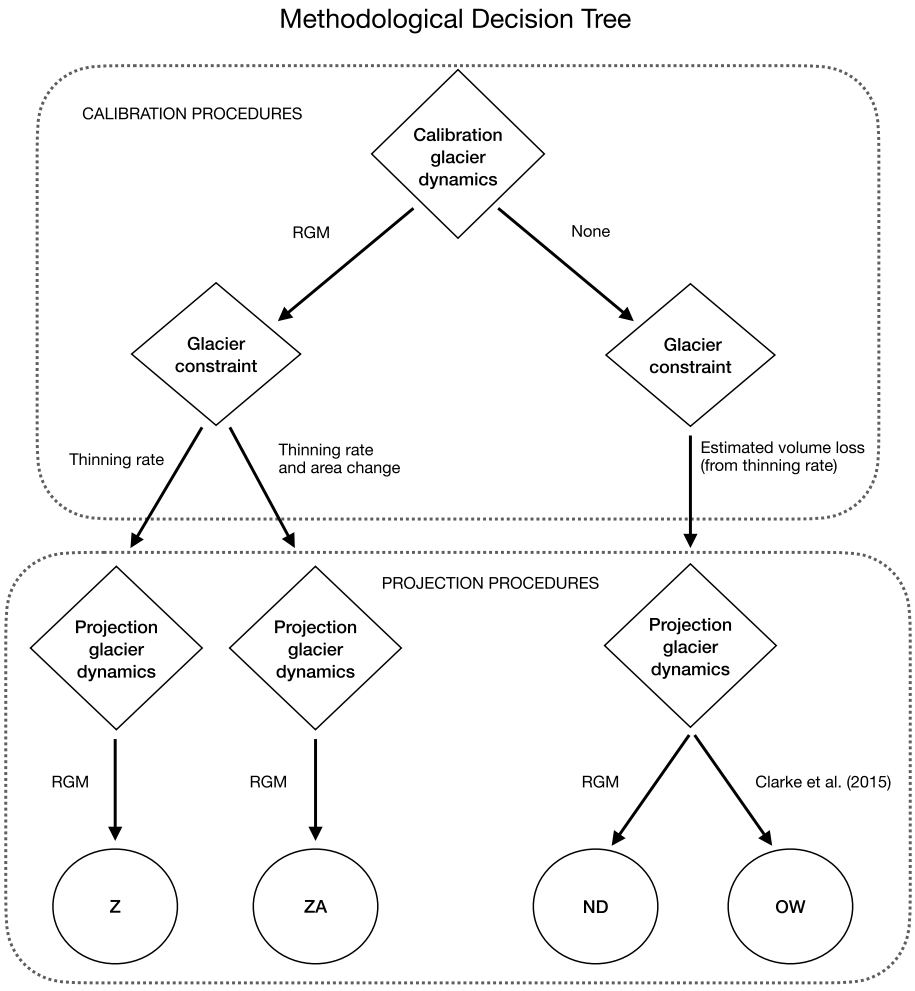

Fig. 1. Decision tree of the calibration/projection choices that lead to OW, ND, Z, and ZA simulations. RGM = regional glaciation model.

hydrological process representations available within the framework and a compatible external glacier dynamics model.

In our study, for each simulated year, changes to glacier coverage are made within Raven on October 1st when snow accumulation and glacier melt are generally thought to be minimal. In the one-way coupling scheme, these changes are dictated by the Clarke et al. (2015) results. In the two-way scheme, ice thickness is updated annually by RGM based on surface mass balance, and corresponding 200 m × 200 m glacier coverage maps are built using a one meter threshold for "glaciated" cells. Raven then updates landcover for the hydrological model by comparing the current glacier coverage map with that of the previous year's.

When an HRU loses its glacier coverage, the landuse type is changed from "glacier" to "barren" and the glacier reservoir within the HRU—which conceptually is depleted—becomes inaccessible. For simplicity, newly barren HRUs are initialized with a soil moisture of zero as simulations show that the hydrology at a basin's outlet is insensitive to this initialization.

Raven's tracer routing feature provides a method for tracking source contributions throughout a simulation; in our study, we use this feature to trace the contribution of glacier melt to streamflow at the basin's outlet. Raven tracks this contribution by treating it as a pollutant that is sourced from glacier melt and is mixed uniformly with other sources of water within all subsequent reservoirs it enters. Pollutants and water from an HRU are routed to the corresponding subbasin's outlet using a discrete transfer function. Subbasin to subbasin routing is determined by iteratively using Newton's root-finding algorithm to solve the discrete form of the reach's storage expression:

$$\frac{V\left(Q_{out}^{n+1}\right) - V\left(Q_{out}^{n}\right)}{\Delta t} = \frac{1}{2}\left(Q_{in}^{n} + Q_{in}^{n+1}\right) - \frac{1}{2}\left(Q_{out}^{n} + Q_{out}^{n+1}\right).$$

Here, Q_{in}^{n} and Q_{out}^{n} are the upstream inflow and the outflow from the subbasin at the end of the nth step and $V(Q)$ is the channel volume for flow rate Q.

2.2.2. UBCWM

All hydrological processes within an HRU are simulated using UBCWM (Quick and Pipes, 1977; Quick, 1995). In its review of hydrological models applied over western Canada, Beckers et al. (2009) identified UBCWM as one of the preferred models for research focused on climate-related changes to mass balance in the region's mountainous and glacierized basins. Like Beckers et al. (2009), we chose UBCWM for this study because it is physically-based and analytically represents snow and glacier melt. Additionally, the model can be run within Raven's interface. UBCWM calculates an HRU's climatic forcings and hydrology using three sub-models: 1) a meteorological sub-model where precipitation is quantified and divided into snow and rain based on climatic forcings, elevation, and atmospheric conditions; 2) a soil sub-model that determines evaporation and distributes the remaining available snow melt and rain into reservoirs representing surface runoff, shallow groundwater, deep groundwater, and interflow based on antecedent conditions; and 3) a routing sub-model that moves water between reservoirs and to the outlet of the HRU. For glacier HRUs the distribution of snow due to the effects of wind and gravity are not

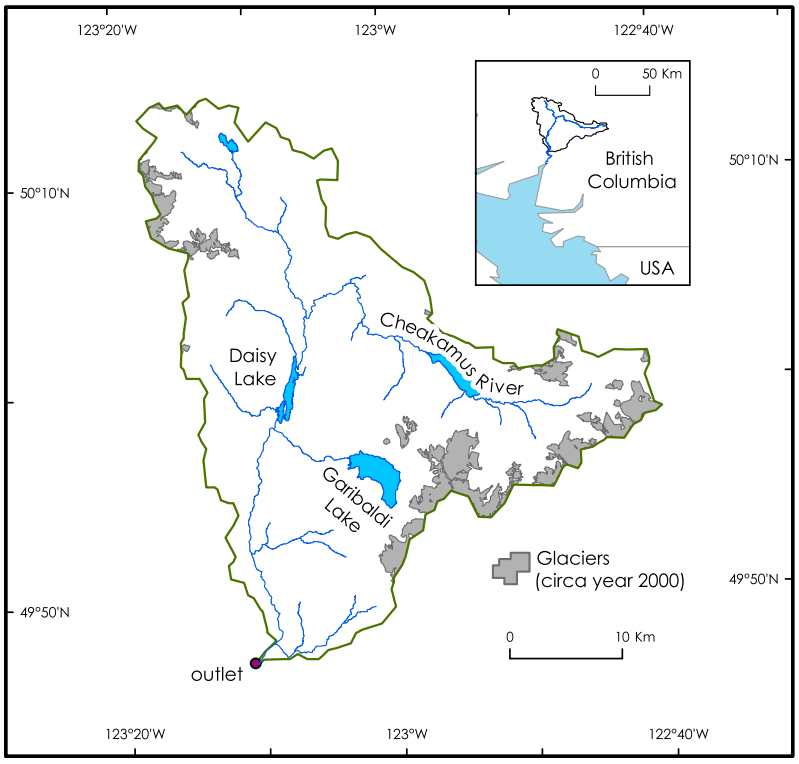

Fig. 2. Cheakamus watershed.

considered and glacier melt is distributed solely to surface runoff.

Typically, UBCWM expects an HRU to be divided into elevation bands that experience different forcings based on orographic corrections to the climatic drivers. Here, we consider the high-resolution HRUs to have uniform elevation. As a result, UBCWM's orographic correction algorithms are not used within a cell, but rather applied to each HRU based on its elevation relative to the 1/16° cell in the forcing data containing the majority of the HRU's area.

2.2.3. RGM

Glacier evolution is modeled using the ice dynamics component of the regional glaciation model (RGM) described in Clarke et al. (2015). This is a two-dimensional vertically-integrated (i.e. 2.5-D) model that assumes the shallow ice approximation and isothermal ice. The equations of the shallow ice model are solved as a non-linear diffusion equation using a super-implicit numerical scheme. Conservation of mass is enforced using a flux-limiting scheme (Jarosch et al., 2013). The model is run on a 200 m × 200 m grid that matches that of the UBCWM simulations, and is forced with annual average surface mass balance and is run at a timestep of 0.2 years.

2.3. Data

For calibration and validation, historical simulations are forced using PNWNAmet (Werner et al., 2019), a 1/16° gridded data set. While operational simulations suggest that climate station forcings may produce better goodness-of-fit results over historical periods (Georg Jost, personal communication, May 12, 2021), we choose to use the gridded PNWNAmet data because of its similarity in structure to the gridded GCM forcings that drive both baseline and future period projections. Simulated streamflow at the outlet is compared to naturalized flows provided by BC Hydro. Simulated glacier volume and area change are evaluated relative to the basin-scale thinning rate and glacier area change values developed in Schiefer et al. (2007) using topographical differences from bias corrected Shuttle Radar Topography Mission data and digital terrain models from aerial photography. Initial glaciers are determined using the estimated subglacial digital elevation maps developed in Clarke et al. (2015) combined with the Terrain Resource Information Management surface digital elevation map (circa 1985) for calibration and the bias corrected Shuttle Radar Topography Mission map (circa 2000) for validation. Glaciers are identified as those cells for which the surface elevation is at least one meter larger than the subsurface elevation. As in Tsuruta and Schnorbus (2021), all other grid cells are assigned a landuse type based on majority area relative to a modified version of the North America Land Cover dataset, edition 2 (Natural Resources Canada/ The Canada Centre for Mapping and Earth Observation, 2013) from the North America Land Change Monitoring System. The original map classifies land use in North America at a 250-m resolution using 19 vegetative classes. In British Columbia, most regions are classified as "temperate or sub-polar needle leaf." To reflect the variation within this class, four sub-classes of "temperate or sub-polar needle leaf" are identified and assigned based on leaf area index from GEOV1 (Baret et al., 2013; Camacho et al., 2013) and vegetative height from Simard et al. (2011).

The Cheakamus Basin's future hydrology under Representative Concentration Pathway 8.5 is simulated using forcing data from six Coupled Model Intercomparison Project Phase 5 global climate models (GCMs): ACCESS1-3, CanESM2, CCSM4, CNRM-CM5, HadGEM2-ES, and MPI-ESM-LR. These GCMs are selected based on their ability to represent model uncertainty in the projections of change in a collection of Western North American climate extremes (Cannon, 2015). The outputs of these GCMs are statistically downscaled to 1/16° using Bias

Corrected/Constructed Analogues with Quantile delta mapping reordering (BCCAQv2; Werner and Cannon (2016)) with PNWNAmet used as the target data set. BCCAQv2 is a hybrid method that combines results from Bias Corrected Constructed Analogs (BCCA; Maurer et al. (2010)) and Quantile Delta Mapping (QDM;Cannon et al. (2015)). BCCA uses spatial aggregation from a linear combination of historical analogues for daily large-scale fields. QDM applies a form of quantile mapping where relative changes in GCM quantiles are preserved to avoid inflationary effects that can occur with standard quantile mapping. BCCAQv2 is an updated version of BCCAQ (version 1), which employed standard quantile mapping. For all of the fully-coupled projections, initial land cover is the same as that of the calibration simulations. From the initial land cover map, glacier coverage can change based on the dynamics simulated by the fully-coupled model. For one-way coupled projections, annual glacier coverage is determined by the results of Clarke et al. (2015). In that study, six possible glacier evolutions were projected based on different GCM forcings; however, Tsuruta and Schnorbus (2021) found the choice of glacier evolution negligible relative to the variation associated with meteorological forcings and parameterization. Hence, we only use one glacier evolution in our one-way coupled projections, which is selected based on its proximity to the median of the evolutionary paths.

2.4. Calibration Procedures

Note: For clarity, here and throughout the paper we use the term **"parameterization"** to refer to a single point in the parameter space of our GHM, i.e. a unique array of parameter values used to simulate the GHM. We use the terms **"set of parameterizations"** or **"parameterization set"** to refer to a collection of such points.

We simulate projections of the future hydrology of the Cheakamus Basin using three separate sets of parameterizations obtained through three different calibration procedures summarized in Table 1 and Fig. 1. The first procedure (ND) is based on the methodology of Jost et al. (2012) and Tsuruta and Schnorbus (2021). The glacier dynamics model is turned off (i.e., only the hydrological model is run during calibration), and the glacier melt simulated over the static glaciers by the hydrological model is constrained based on thinning rates converted to mass balance. Although the results of Tsuruta and Schnorbus (2021) suggest that streamflow properties are insensitive to the precise path of glacier area dynamics within a prescribed range, we nonetheless wish to explore the effects of running the fully-coupled model (with glacier dynamics on) during the calibration period because a) it allows for direct constraint of glacier melt based on thinning rates, and b) the internal dynamics model may produce a range of glacier dynamics much larger than the one studied in Tsuruta and Schnorbus (2021). Hence, in the second procedure (Z), we follow studies such as Ismail et al. (2020), Meyer et al. (2019) and Lutz et al. (2016) and run the fully-coupled model during calibration with glacier melt constrained directly based on observed versus simulated thinning rates. Our third procedure (ZA) follows the Z methodology, but constrains glacier melt by both observed thinning rates and observed surface area change to minimize the compensating effects of errors within these two properties.

Table 1
Calibration and projection procedures.

Set	CalibrationGlacier dynamics	Glacier metrics	Validation/ ProjectionGlacier dynamics
ND	Static glacier	bell-shaped membership function	RGM
OW[a]	Static glacier	bell-shaped membership function	(Clarke et al., 2015) results
Z	RGM	Absolute error in thinning rate	RGM
ZA	RGM	Absolute error in thinning rate and area change	RGM

[a] The parameterization set for one-way coupled (OW) projections is the same as the ND parameter set.

Rather than generate a separate set of parameterizations for the one-way projections, we use the ND parameterization set. The ND calibration procedure varies slightly from that of Tsuruta and Schnorbus (2021) in that its glacier coverage is static during the entire simulation whereas glacier coverage in Tsuruta and Schnorbus (2021) is switched mid-way through the calibration period from glacier observations circa the first year of simulation to glacier observations circa the last year of simulation. We use the ND set for one-way simulations 1) to save on computational cost, 2) because observed Cheakamus glacier area change from 1985–1999 is minimal (< 1 km^2), and 3) to directly analyze the effects of one-way versus two-way coupling on hydrological projections.

Calibration simulations for all of the procedures are for 1985–1999 (water years). While this period is small relative to the timescale of glacier dynamics, it was chosen based on the availability of glacier volume and area change observations, a common limiting factor in calibration (Naz et al., 2014). For each of the procedures, the non-dominated sorting genetic algorithm II (Deb et al., 2002) is used to find Pareto optimal parameterizations consisting of 15 calibrated parameters. These parameters were selected based on a sensitivity analysis and are allowed to vary within ranges determined by a combination of prescription from Quick and Pipes (1977), internal BC Hydro UBCWM simulations of the Cheakamus (Georg Jost, personal communication, May 12, 2021), and the authors' experience calibrating UBCWM in Tsuruta and Schnorbus (2021). In the optimization algorithm, points in the parameter space are evaluated based on a multi-objective function composed of each calibration procedure's specific glacier metrics and the following four streamflow metrics: Nash–Sutcliffe Efficiency, Nash–Sutcliffe Efficiency of the log of streamflow, percent bias, and Kling-Gupta efficiency. The uniform, basin-wide thinning rate in Z is constrained using the absolute error metric. In ZA, the thinning rate and the glacier surface area change are constrained using absolute error. For ND we follow the procedure described in Tsuruta and Schnorbus (2021): because no simulated thinning rate is available, we first make upper (b_u) and lower (b_l) estimates of glacier net mass balance based on observed thinning rates, the uncertainty associated with those observations (± 3 m, Schiefer et al. (2007)), and the uncertainty in the glaciers' bulk density (Dyurgerov et al., 2009; Huss, 2013):

$$b_l = min\{0.7(\Delta H - 3), 0.85(\Delta H - 3)\} \quad (1)$$

$$b_u = max\{0.7(\Delta H + 3), 0.85(\Delta H + 3)\}, \quad (2)$$

where, ΔH is average change in glacier height across the basin in meters. We then constrain simulated mass balance b_s using a bell-shaped membership function (Zhao and Bose, 2002)

$$BMF_B = \frac{1}{1 + \left|\frac{b_s - b_m}{b_u - b_l}\right|^2}, \quad (3)$$

where b_m is the midpoint between b_u and b_l. Because the optimization algorithm is designed to find Pareto optimal (i.e. "non-inferior") solutions, each metric in a given set of constraints is considered to have equal weight.

The calibration algorithm is iterated 30 times, and generates 60 parameterizations each iterate. After the final iteration, we verify that the algorithm has "converged" in the sense that each of the 60 parameterizations is Pareto optimal. For each calibration procedure, a subset of six of the 60 Pareto optimal parameterizations are selected for validation and projections based on combined metric performance. Validation is based on performance against streamflow observations over the 2000–2008 (water year) period.

2.5. Projection Procedures

Using the sets of parameterizations from the ND, Z, and ZA calibration procedures, we project the Cheakamus Basin's future hydrology under Representative Concentration Pathway 8.5 from 1981 through 2098 using the fully-coupled model described in Section 2.2. For the one-way coupling projections described in Section 2.2, we use the parameterization set from the ND procedure. In all subsequent sections, we refer to the one-way projections that use the ND parameterization set as "OW" projections and refer to the fully-coupled projections as "ND".

2.6. Analysis

2.6.1. Variability within Pareto optimal sets

We wish to compare between the different calibration/projection procedures the ability of the optimization algorithm to constrain parameter values, as well as the procedure's ability to constrain the following model outputs: 1) summer (July-August) streamflow Q, 2) the glacier contribution to summer streamflow Q_G, 3) summer seven-day low flow Q_{LF}, and 4) the coefficient of variation of annual summer streamflow CV_Q. To this end, for a given calibration procedure and parameter, we compute amongst its 60 Pareto optimal values the standard deviation normalized as a percentage of the parameter's upper limit value. This normalized value is computed for each parameter and procedure. To assess variability in model output amongst the Pareto optimal sets, we use each projection procedure to simulate the validation period for all 60 of its Pareto optimal parameterizations. We then test for differences in variance amongst the sets using an F-sigma test with $\alpha = 0.05$. This is the only analysis where all 60 Pareto optimal parameterizations are studied. In all other analysis, a subset of six parameterizations is used.

2.6.2. Variability from forcing set versus parameterization set

For each procedure, we also wish to compare the variability in model outputs that stems from the set of six selected UBCWM parameterizations (P) to that which stems from the set of six GCMs (F). As in Tsuruta and Schnorbus (2021), we make this comparison for our four properties of interest by calculating the "between to within variability ratio" for both the set of parameterizations and the set of forcings. To calculate this ratio for the set of forcings and model output Q, time-averaged summer streamflow $\overline{Q}$ was computed for each simulation, producing a set of 36 average values $S = \{\overline{Q}_{(f,p)}\}_{(f,p)\in F\times P}$. This set was then separated into six groups. The first group contains the six projections that use the first set of climate forcings ($F_1 = \{\overline{Q}_{(f_1,p)}\}_{(p)\in P}$), the second group contains the six projections that use the second set of forcings ($F_2 = \{\overline{Q}_{(f_2,p)}\}_{(p)\in P}$), and so on. For each F_i, the mean value of the group is computed and the "between group variability" (BV_F) set to the variance between these means. Next, the variance within each group F_i is computed and the results are averaged to calculate the "within group variability" (WV_F). The "between to within variability ratio" is the ratio of the between group variability and the within group variability

$$BWR_F = \frac{\mathrm{BV}_F}{\mathrm{WV}_F}.$$

Analogous procedures are used to calculate the ratio for the set of parameterizations and the other model outputs. For a given streamflow property, we consider factors with a relatively large between to within variability ratio to have a relatively large contribution to variance of the streamflow property.

2.6.3. Variability of changes between end-century and baseline

For each set of projections (OW, ND, Z, and ZA), we calculate the change from baseline (1981–2008) to end-century (2071–2098) of time-averaged values of summer streamflow, glacier contribution to summer streamflow, summer seven-day low flow, and the CV of summer streamflow. We assess the variability of these changes between OW, ND, Z, and ZA in three ways: first, we test for significance in the projected changes of each procedure using Welch's unequal variances t-test (Welch, 1947) with $\alpha = 0.05$ and look for any differences between the procedures. Second, we use the same t-test to check for significant differences in magnitude between the changes from baseline to end-century projected by OW, ND, Z, and ZA. Finally, we perform a two-way analysis of variance (ANOVA) and calculate the relative effect sizes of 1) GCM forcings and 2) calibration/projection procedures on the projected differences between baseline and end-century values.

3. Results

3.1. Historic period: 1985–2008

3.1.1. Calibration and validation

Calibration and validation performance of the six selected Pareto optimal parameterizations was similar across all three procedures (Table 2). Metric scores over the calibration and validation periods are reasonable, though the models generally struggled to capture low flow winter conditions as well as peak extremes (Fig. 3). Over the calibration period, daily Nash–Sutcliffe Efficiency values ranged from 0.57–0.64, percent bias between 2.8–5.6%, Nash–Sutcliffe Efficiency of the log of streamflow between 0.57–0.65, and Kling-Gupta Efficiency between 0.52–0.62. Over the validation period, daily Nash–Sutcliffe Efficiency was within 0.58–0.64, percent bias ranged from 9.6–12.4%, Nash–Sutcliffe Efficiency of the log of streamflow ranged from 0.56–0.63, and Kling-Gupta Efficiency varied within 0.58–0.63. While higher goodness-of-fit metric scores are preferable, we consider our results adequate for the purposes of our study.

3.1.2. Pareto optimal set variability

The results from computation of each calibrated parameter's normalized standard deviation within its 60 Pareto optimal values are mixed (Table 3). There is no clear trend regarding the relative magnitude of the normalized values when comparing between calibration procedures. However, amongst the highest sensitivity parameters (determined using Morris method analysis) it appears that the distribution of Pareto optimal values using procedure Z is generally tightest, with the next tightest distribution being produced by procedure ZA, and the least tightest by procedure ND. In particular, the exponential parameter that determines the rate of albedo decay for non-glacierized and glacierized cells (P0ALBMLX and $\mathrm{P0ALBMLX}_G$) appears to be best

Table 2
Average performance results over the calibration period (1985–1999 water years) for each calibration procedure's full set of sixty Pareto optimal parameterizations and the selected subset of six parameterizations. NSE = Nash–Sutcliffe Efficiency. LNSE = log of NSE. PBIAS = percent bias. KGE = Kling-Gupta Efficiency. MBF = membership bell function. $E(\Delta H)$ = absolute error in glacier thickness change (m). $E(\Delta A)$ = absolute error in glacier area change (km^2).

	Streamflow metrics				Glacier metrics		
Full set	NSE	LNSE	PBIAS	KGE	MBF	$E(\Delta H)$	$E(\Delta A)$
ND	0.61	0.62	8	0.64	0.62	-	-
Z	0.61	0.62	8	0.64	-	1.26	-
ZA	0.60	0.61	9	0.65	-	1.55	24

	Streamflow metrics				Glacier metrics		
Subset	NSE	LNSE	PBIAS	KGE	MBF	$E(\Delta H)$	$E(\Delta A)$
ND	0.61	0.62	4	0.60	0.54	-	-
Z	0.59	0.59	4	0.59	-	0.26	-
ZA	0.59	0.59	4	0.60	-	0.32	4

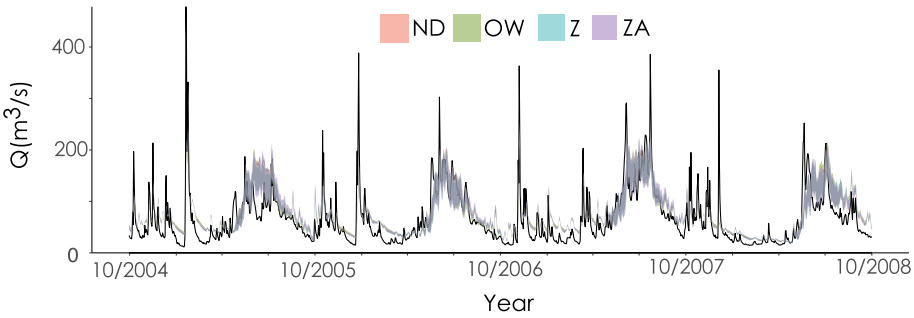

Fig. 3. Hydrograph of simulated and observed streamflow over part of the validation period (2005–2008 WY).

Table 3
Standard deviations for each calibration procedure of every calibrated parameter across their 60 Pareto optimal values normalized by parameter value upper limit.

Parameter	Description	ND	Z	ZA
POROSITY	Porosity of soil	4	6	5
$PERC_M$	Maximum capacity of sub-surface storage	7	11	12
P0GRADU	Precipitation gradient factor for high elevations	18	14	15
P0DZSH	Deep zone share time constant	11	12	13
$IMPERM_F$	Maximum impermeable fraction of FOREST landclasses	3	1	1
$IMPERM_S$	Maximum impermeable fraction of GRASS/SHRUBLAND landclasses	1	1	1
SWI	Maximum liquid snow storage capacity as a fraction of snowpack SWE	15	12	8
A0STAB	Precipitation gradient modification factor (non-glacierized cells)	33	39	30
P0ALBASE*	Albedo less than which decay is non-linear (non-glacierized cells)	4	5	5
P0ALBMLX*	Albedo decay parameter (non-glacierized cells)	28	23	26
$A0STAB_G$	Precipitation gradient modification factor (glacierized cells)	348	376	177
$P0ALBASE^*_G$	Albedo less than which decay is non-linear (glacierized cells)	8	8	7
$P0ALBMLX^*_G$	Albedo decay parameter (glacierized cells)	26	10	23
$P0ALBMIN_G$	Albedo of a very aged snowpack (glacierized cells)	4	3	7
$A0TERM_G$	Maximum daily temperature range (glacierized cells)	14	14	12

* indicates a high sensitivity parameter.

constrained by procedure Z.

Analysis of the variability of each projection procedure's full set of 60 Pareto optimal parameterizations over the validation period show no significant differences between the procedures in constraining simulated summer streamflow (Table 5). With the exception of the Z-ZA pairing, there was also no significant difference between the CV_Q variance simulated by the procedures, though the magnitude of OW's simulated CV_Q appears to be larger than that of the others (Fig. 5).

3.2. Projections: 1981–2098

Summer projection results from OW, ND, Z, and ZA are generally consistent with one another as well as with the conceptual model of increasing radiative forcings leading to an earlier spring onset of snowmelt and a resulting decrease in summer streamflow (Table 4). In conjunction with this loss of summer snowmelt, simulations of glacier dynamics, though varied, all project nearly total glacier loss by the end-century (Fig. 4). Correspondingly, the simulations consistently project a loss of glacier contribution to streamflow over the summer period.

3.2.1. Forcing set versus parameterization set variability

Table 6 shows the results of the between to within variability ratio calculations for all projection sets ($N = 6{\cdot}\text{GCMs} \times 6{\cdot}\text{parameterizations} = 36$) for each calibration/projection procedure. For each procedure, the majority of the variability in summer streamflow, the seven-day summer low flow, and summer streamflow CV appear to result from variability in forcings rather than from variability in the procedure's subset of Pareto optimal parameterizations. Variability in the Z and ZA projections of the glacier component of summer streamflow also appear to be mostly a result of variability in forcings. For the OW and ND procedures, more of the variability in the glacier contribution to summer streamflow stems from variability in the subset of parameterizations.

3.2.2. Variability in projected changes

The sign and significance of projected changes agree across all projection procedures (Table 4). For each set, summer streamflow, the glacier contribution to summer streamflow, and the summer seven-day low flow are all expected to decrease in the end-century, while the CV of summer streamflow is expected to increase. Though the sign and significance of these changes are consistent among OW, ND, Z, and ZA;

Table 4
Mean across 36 projections of total (Q), glacier (Q_G), and low flow (Q_{LF}) summer runoff and CV of Q (CV_Q) for each calibration procedure. Δ-End represent the difference between baseline (1981–2005) and end-century (2071–2098) values. Positive values indicate an increase from baseline.

	Q (m^3/s)				Q_G(m^3/s)			
Era	OW	ND	Z	ZA	OW	ND	Z	ZA
Baseline	83	85	92	92	7	9	7	7
Δ-End	−53[a]	−47[a]	−52[a]	−53[a]	−7[a]	−8[a]	−6[a]	−7[a]

	Q_{LF} (m^3/s)				CV_Q			
Era	OW	ND	Z	ZA	OW	ND	Z	ZA
Baseline	28	28	29	29	0.16	0.16	0.16	0.15
Δ-End	−12[a]	−7[a]	−7[a]	−7[a]	0.12[a]	0.04[a]	0.05[a]	0.06[a]

[a] changes from baseline are statistically significant at $\alpha = 0.05$.

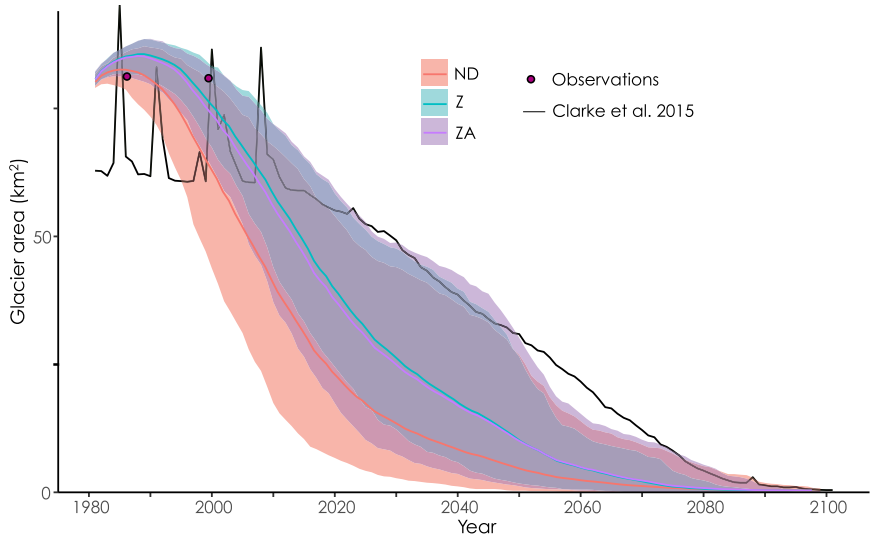

Fig. 4. Spreads and means of simulated glacier area evolution. Initial differences between Clarke et al. (2015) results and GHM simulated glaciers are a result of different initialization (circa 1985 observed glaciers for ND, Z, and ZA, and simulated 1985 glaciers for Clarke et al. (2015)).

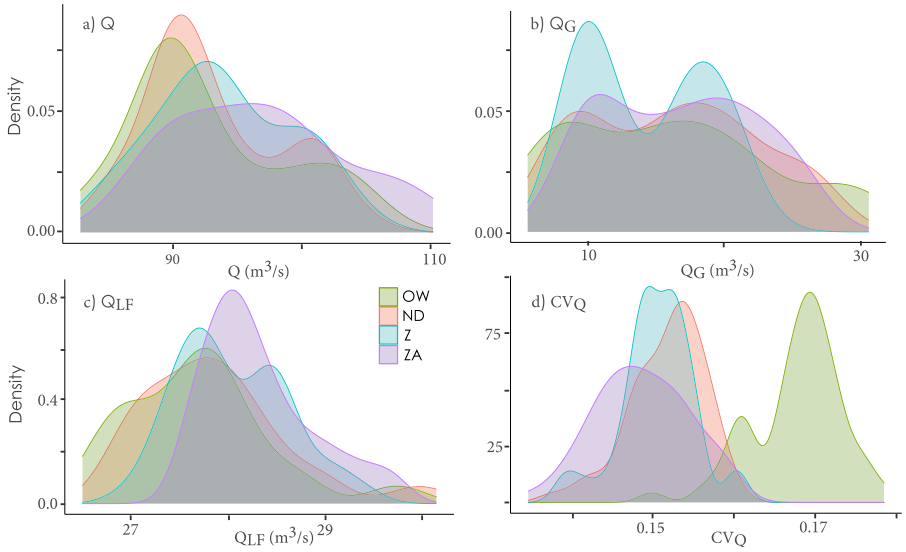

Fig. 5. Gaussian density estimate across each calibration/projection procedure's 60 Pareto optimal parameterizations of time-averaged summer properties a) total seasonal discharge, b) glacier contribution to streamflow, c) seven-day low flow, and d) the CV of streamflow over the validation period (2000–2008 WY). $N = 60$ for each distribution.

Table 5
Variance values over the validation period (2000–2008 WY) across each projection procedure's 60 Pareto optimal parameterizations. S or – in (i, j) position indicates statistically significant (S) or insignificant (–) difference in variance between projection procedures corresponding to row i and column j. Significance level $\alpha = 0.05$

	Q (m³/s)				Q_G(m³/s)			
	σ^2(m⁶/s²)	ND	Z	ZA	σ^2(m⁶/s²)	ND	Z	ZA
OW	37	–	–	–	54	–	S	S
ND	27		–	–	38		S	–
Z	29			–	21			–
ZA	43				30			
	Q_{LF} (m³/s)				$CV_Q \cdot 10^5$			
Cal	σ^2 (m⁶/s²)	ND	Z	ZA	σ^2	ND	Z	ZA
OW	.55	–	S	S	2.1	–	–	–
ND	.56		S	S	3.0		–	–
Z	.32			–	2.0			S
ZA	.32				3.4			

Table 6
"Between" to "within" variability ratios (BWR) for Q, Q_G, Q_{LF}, and CV_Q over 2010–2098. P = set of parameterizations ($P = 6$), F = set of forcings ($F = 6$).

	BWR Q				BWR Q_G			
Set	OW	ND	Z	ZA	OW	ND	Z	ZA
P	0.1	0.2	0.3	0.3	1.3	6.1	0.4	0.6
F	10.3	4.1	2.8	2.9	0.6	0.2	2.2	1.5
	BWR Q_{LF}				BWR CV_Q			
Set	OW	ND	Z	ZA	OW	ND	Z	ZA
P	0.1	0.2	0.1	0.1	0.1	0.2	0.3	0.3
F	7.4	5.2	17.9	7.5	11.2	5.6	2.8	2.8

Table 7
Statistically significant (S) and insignificant (–) differences in the mean of projected changes across 36 projections to total (Q), glacier (Q_G), and low flow (Q_{LF}) summer runoff and CV of Q (CV_Q) amongst the calibration/projection procedures. Significance level $\alpha = 0.05$

	Q (m^3/s)			Q_G(m^3/s)		
Cal	OW	ND	Z	OW	ND	Z
ND	S			S		
Z	–	S		–	S	
ZA	–	S	–	–	S	–
	Q_{LF} (m^3/s)			CV_Q		
Cal	OW	ND	Z	OW	ND	Z
ND	S			S		
Z	S	–		S	–	
ZA	S	–	–	S	–	–

the mean and distribution of the expected changes show some variation between projection procedures (Fig. 6). Analysis of the magnitude of projected changes shows statistically significant differences between the calibration/projection procedures (Table 7). The magnitude of changes to summer streamflow and glacier melt projected by the two-way ND procedure is significantly different from the other two-way methods and the one-way method. The magnitude of changes to summer low flow and CV projected by one-way coupling are significantly different from those projected by the two-way methods. The apparent difference in projected summer seven-day low flow between OW and the other projection procedures can also be seen in the range of flow duration curves for each procedure (Fig. 7).

Two-factor ANOVA shows both forcings and projection procedures explain a significant ($\alpha = 0.05$) amount of variation in the projected differences of all four computed variables. With the exception of summer streamflow, the variations explained by calibration/projection procedure are as large or larger than those explained by GCM (Fig. 8).

4. Discussion

Calibration and validation simulations demonstrate that the GHM can reasonably reproduce historic streamflow in the Cheakamus Basin (Table 2). Still, some biases, particularly in baseflow, exist (Fig. 3) and higher goodness-of-fit measures are preferable. Our goodness of fit values may be a symptom of the difficulty inherit in parameterizing a model to simultaneously fit both the basin's streamflow and glacier observations, as well as the underlying deficiencies in model structure and input data. This struggle to precisely fit observations may lead to higher variability within a procedure's Pareto optimal parameterizations. Though the calibration procedures' performances against observations were similar and our analysis of variability is comparative amongst the procedures rather than absolute, our results should nonetheless be interpreted with this limitation in mind.

Over the validation period, the models calibrated using the fully coupled GHM produced tighter overall constraints on the Cheakamus Basin's streamflow properties (Table 5). Compared to OW, Z and ZA both displayed significantly smaller variance in glacier contribution to summer streamflow and seven-day low flow. Compared to ND, Z's variance in both summer streamflow and seven-day low flow was significantly smaller, while ZA's variance was only significantly smaller in seven-day low flow. In none of the four properties analyzed was the variance in the ND or OW sets significantly smaller than those of Z and ZA. While the fully coupled calibration procedures performed better in terms of variance than their static counterpart, the additional constraint on glacier area that defines the difference between Z and ZA does not appear to positively influence calibration results. The ZA set's variance was not significantly smaller than that of Z for any of the analyzed properties, while the Z set showed a significantly smaller variance than ZA in the coefficient of variation in summer streamflow.

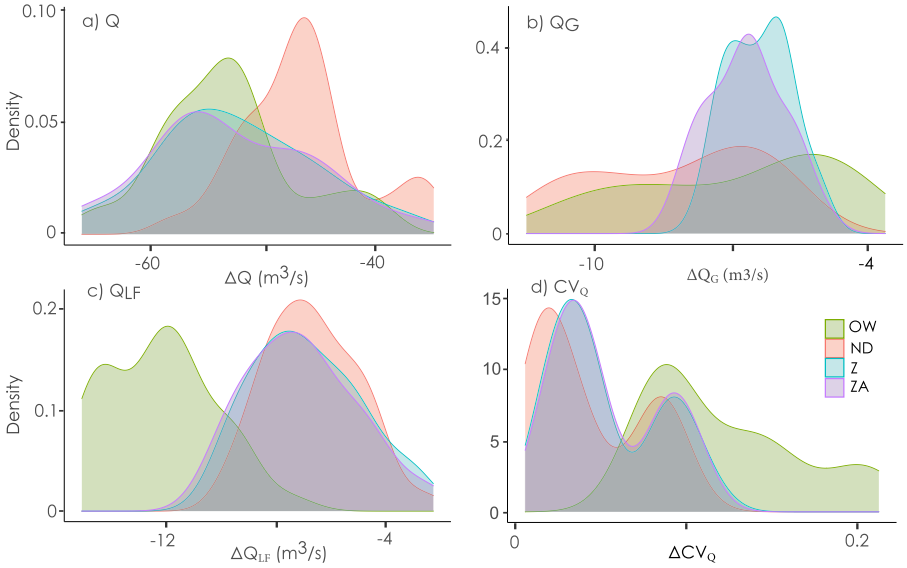

Fig. 6. Gaussian density estimate of projected differences from baseline (1981–2005) to end–century (2071–2098) in the magnitude of summer properties a) total seasonal discharge, b) glacier contribution to streamflow, c) seven-day low flow, and d) the CV of discharge for each calibration/projection procedure's 36 simulations. $N = 36$ for each distribution.

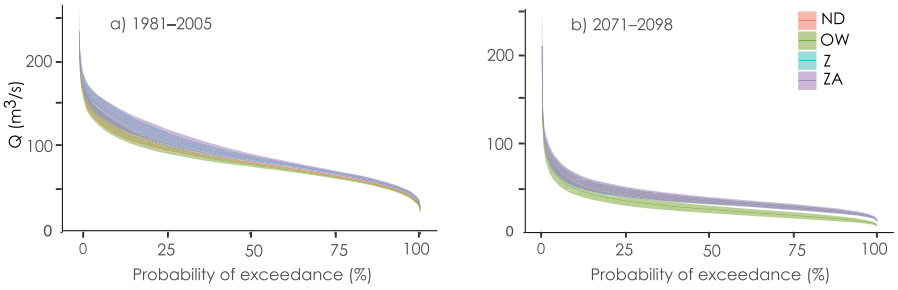

Fig. 7. Summer flow duration curves for a) baseline and b) end–century eras.

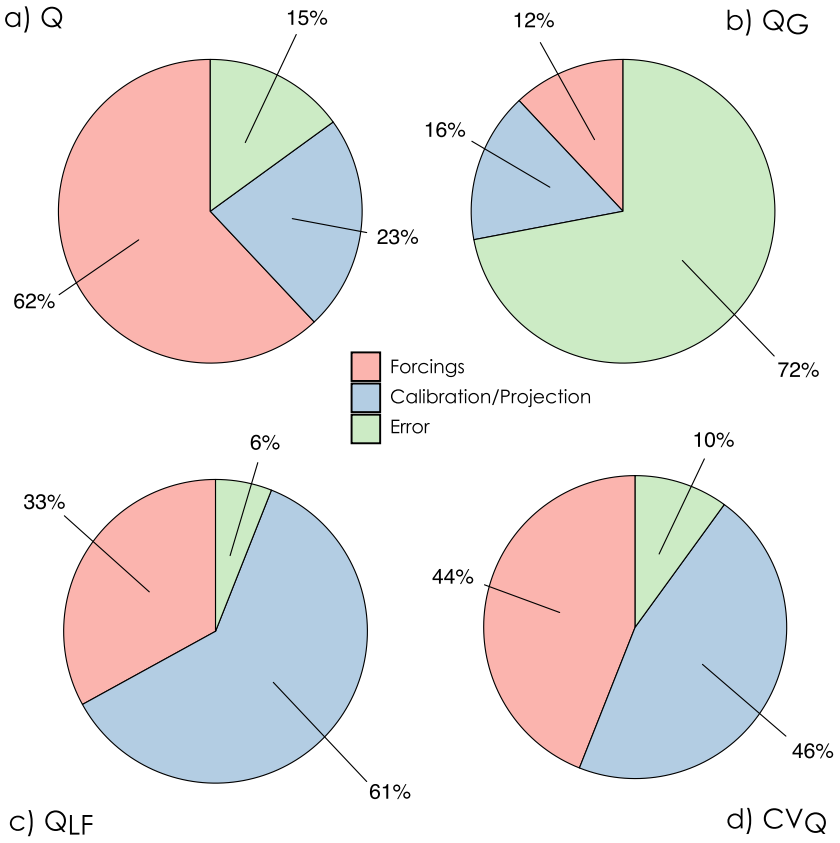

Fig. 8. Effect sizes of forcings and calibration/projection procedures on changes from baseline to end-century of a) summer streamflow, b) glacier contribution to summer streamflow, c) seven-day summer low flow, and d) the CV of summer streamflow. "Error" refers to the percent of total variability that cannot be explained by variability in forcings or calibration/projection procedures. Effects of both factors are statistically significant for all variables at $\alpha = 0.05$.

These results imply that there is a benefit to parameterizing a GHM using dynamics during the calibration period. For those GHMs that calibrate to thinning rate, our results do not imply any benefit from the additional constraint of glacier area. Our analysis of the normalized standard deviation of individual parameters amongst their Pareto optimal sets generally agree with this conclusion, as calibration procedure Z, followed next by ZA, best constrains the highest sensitivity parameters (Table 3). These parameters control the evolution of albedo as a snowpack ages and therefore have a direct influence on snow melt, glacier melt, and mass balance—the primary input for the glacier dynamics model.

Conceptually, one would expect constraining glacier area to be beneficial to a model, as it helps to avoid internal compensation for errors in the melt rate with errors in glacier area change. However, our results do not display any evidence of such a compensating effect as the glacier area evolutions in the Z and ZA projections are generally very similar (Fig. 4). The absence of any benefit from the addition of an area constraint may relate to the relatively short calibration period during which glacier area change was essentially zero. It is possible that the basin's glaciers were sufficiently thick during this period that smaller errors in melt rate were unable to manifest as glacier area errors. Such limitations stemming from the availability of glacier observations are common in this field, but should nonetheless be kept in mind when interpreting our study's results.

The magnitude of projected changes in the Cheakamus Basin are found to vary significantly among the projection procedures. Z and ZA,

the two fully-coupled projection sets that are calibrated using the fully-coupled model, show agreement between one another. The magnitudes of changes in summer streamflow and its glacier contribution projected by ND varied from those of the other procedures (Table 7). Although simulated changes in summer streamflow glacier contribution Q_G for OW are not significantly different from those of Z and ZA, the one-way procedure's projection set's distribution of ΔQ_G appears to more closely resemble that of ND and have a larger variance than ΔQ_G for Z or ZA (Fig. 6). Results show OW simulations projecting a significantly larger decrease in summer seven-day low flow Q_{LF} and increase in the CV of summer streamflow than the ND, Z, and ZA procedures (Table 7). The difference in ΔQ_{LF} appears to be a result of a difference in projected end-century Q_{LF} as baseline flow duration curves are similar for OW, ND, Z, and ZA; whereas the end-century OW curve appears to separate from the other procedures at the flow values with a high probability of exceedance (Fig. 7).

ANOVA shows that choice of projection/calibration procedure accounts for a significant amount of the variation in the projected changes of all four computed streamflow variables. The effect size computations quantify this contribution and show that the variation attributable to the choice of projection/calibration procedure is as large or larger than what can be attributed to the choice of forcing for glacier contribution to streamflow, seven-day summer low flow, and the coefficient of variation of summer streamflow (Fig. 8). In previous studies examining uncertainties in hydrological projections under climate change (e.g. Kay et al., 2009; Prudhomme and Davies, 2009; Prudhomme and Davies, 2009; Najafi et al., 2011), choice of GCM has generally been found to be the largest source of uncertainty in the modelling chain. However, these studies did not consider parameterization variation uncertainty due to calibration procedure, but rather compared the variation due to GCM structure against the internal variability of the hydrological model associated with its structure and parameters. That we find the uncertainty associated with calibration/projection procedure to be comparable to this previously established large source of uncertainty underscores the importance of calibration uncertainty in interpreting the results of GHMs.

Despite their differences, all four projection sets are consistent in their broad conclusions regarding the Cheakamus Basins' future hydrology: the basin's glaciers melt, summer streamflow decreases, and CV increases (Table 4). This would appear to imply that the projected changes in climate forcings are strong enough to make the sign and significance of changes to Cheakamus Basin's hydrology insensitive to the calibration and projection procedures explored in this study. In some ways, this insensitivity is unsurprising—the rapid thinning rates and area loss (Schiefer et al., 2007; Moore et al., 2009) observed in British Columbia, combined with the general expectation of a warmer future climate would seem to indicate that, irrespective of trajectories, simulated glacier evolutions will inevitably end in large-scale loss. Still, while such a result may be intuitive, it is not obvious *a priori*. Calibration of glacier dynamics was performed not only to accurately simulate glacier evolution, but also to constrain the non-glacier parameters and thereby avoid poor parameterizations that perform well historically because of the compensating effects between glacierized and non-glacierized parts of the basin. We assert that the overall impact of this secondary benefit of glacier calibration on projections is generally unclear prior to simulation.

5. Conclusions

In this study, we presented a new, adaptable, fully-coupled glacio-hydrological modelling system developed within a modular framework. Our fully-coupled GHM was used to analyze the impact of differing calibration procedures on hydrological projections of the Cheakamus Basin. We additionally compared these projection sets to simulations wherein glacier dynamics are prescribed using the results of Clarke et al. (2015).

Our results indicate that the climatic forcings projected under Representative Concentration Pathway 8.5 have sufficient strength to make the sign and significance of changes to the basin's summer hydrology insensitive to variation between our selected calibration and projection procedures. Variation between our calibration/projection procedures does however appear to have an impact on the magnitude of projected changes (Table 4) and can be a source of uncertainty comparable to known sources of large uncertainty such as GCM structure (Fig. 8). This would imply that while some facets of glacier dynamic modelling—such as the critically limiting availability of observations—inevitably lead to uncertainty in projections, there is still room to reduce the uncertainty in GHM projections.

To this end, though projected changes from each methodology cannot be compared to observations, we nonetheless identify a preferred procedure for the new GHM based on three principles: 1) An internally consistent model is preferable to a model without internal consistency. 2) It is desirable for a calibration procedure to minimize variations in output between optimal parameterizations. 3) A methodology with fewer data requirements is preferable to one with more. Accordingly, we favor the fully-coupled model, calibrated with glacier dynamics and thinning rates as a target observation (method Z) for projecting hydrology in a partially glacierized basin as it is the fully-coupled model with the fewest data requirements and also leads to the tightest overall constraint of the four streamflow properties analyzed (Tables 3, 5).

Our study has been primarily focused on one fully-coupled GHM applied to a single site with limited observations. We therefore do not recommend a direct application of our findings to other glacio-hydrological studies. Rather, we suggest viewing our work as an example highlighting the importance of calibration techniques and their associate uncertainties in GHM simulations. Based on our findings, we advocate additional research involving a variety of models, study sites, and observations is needed to better codify best practices for GHM calibration/projection.

CRediT authorship contribution statement

Kai Tsuruta: Conceptualization, Methodology, Software, Formal analysis, Investigation, Writing - original draft, Writing - review & editing, Visualization. **Markus A. Schnorbus:** Conceptualization, Writing - review & editing, Supervision, Project administration.

Declaration of Competing Interest

The authors declare the following financial interests/personal relationships which may be considered as potential competing interests: Kai Tsuruta reports financial support was provided by the Global Water Futures project. Study site was suggested by Georg Jost of BC Hydro.

Data availability

Data will be made available on request.

Acknowledgments

This study was partially funded by a grant from Global Water Futures project, funded by the Canada First Research Excellence Fund. We thank BC Hydro's Georg Jost for suggesting our study basin and lending his expertise regarding calibration of the Cheakamus. We thank Francis Zwiers for his internal review of this manuscript and two anonymous reviewers for their insightful comments.

References

Baret, F., Weiss, M., Lacaze, R., Camacho, F., Makhmara, H., Pacholczyk, P., Smets, B., 2013. GEOV1: LAI, FAPAR Essential Climate Variables and FCover global times series capitalizing over existing products. Part1: Principles of development and production. Remote Sens. Environ. 137, 299–309.

Barnett, T., Adam, J., Lettenmaier, D., 2005. Potential Impacts of a Warming Climate on Water Availability in Snow-Dominated Regions. Nature 438, 303–309.
Beckers, J., Smerdon, B., Wilson, M., 2009. FORREX Review of hydrologic models for forest management and climate change applications in British Columbia and Alberta. FORREX, Kamloops, BC, oCLC, p. 837223088.
Blöschl, G., Montanari, A., 2010. Climate change impacts—throwing the dice? Hydrol. Process. 24 (3), 374–381.
Bolch, T., Menounos, B., Wheate, R., 2010. Landsat-based inventory of glaciers in western Canada, 1985–2005. Remote Sens. Environ. 114 (1), 127–137.
Brown, L.E., Hannah, D.M., Milner, A.M., 2005. Spatial and temporal water column and streambed temperature dynamics within an alpine catchment: implications for benthic communities. Hydrol. Process. 19 (8), 1585–1610.
Camacho, F., Cernicharo, J., Lacaze, R., Baret, F., Weiss, M., 2013. GEOV1: LAI, FAPAR essential climate variables and FCOVER global time series capitalizing over existing products. Part 2: Validation and intercomparison with reference products. Remote Sens. Environ. 137, 310–329.
Cannon, A.J., 2015. Selecting GCM Scenarios that Span the Range of Changes in a Multimodel Ensemble: Application to CMIP5 Climate Extremes Indices. J. Clim. 28 (3), 1260–1267.
Cannon, A.J., Sobie, S.R., Murdock, T.Q., 2015. Bias Correction of GCM Precipitation by Quantile Mapping: How Well Do Methods Preserve Changes in Quantiles and Extremes? J. Clim. 28 (17), 6938–6959.
Clarke, G.K.C., Jarosch, A.H., Anslow, F.S., Radić, V., Menounos, B., 2015. Projected deglaciation of western Canada in the twenty-first century. Nat. Geosci. 8 (5), 372–377.
Craig, J.R., Brown, G., Chlumsky, R., Jenkinson, R.W., Jost, G., Lee, K., Mai, J., Serrer, M., Sgro, N., Shafii, M., Snowdon, A.P., Tolson, B.A., 2020. Flexible watershed simulation with the Raven hydrological modelling framework. Environ. Modell. Softw. 129, 104728.
Deb, K., Pratap, A., Agarwal, S., Meyarivan, T., 2002. A fast and elitist multiobjective genetic algorithm: NSGA-II. IEEE Trans. Evol. Comput. 6 (2), 182–197.
Dyurgerov, M., Meier, M.F., Bahr, D.B., 2009. A new index of glacier area change: A tool for glacier monitoring. J. Glaciol. 55, 710–716.
Fountain, A.G., Tangborn, W.V., 1985. The effect of glaciers on streamflow variations. Water Resour. Res. 21 (4), 579–586.
Frans, C., Istanbulluoglu, E., Lettenmaier, D.P., Naz, B.S., Clarke, G.K.C., Condom, T., Burns, P., Nolin, A.W., 2015. Predicting glacio-hydrologic change in the headwaters of the Zongo River, Cordillera Real. Bolivia. Water Resour. Res. 51 (11), 9029–9052.
Gardner, A., Moholdt, G., Cogley, J., Wouters, B., Arendt, A., Wahr, J., Berthier, E., Hock, R., Pfeffer, W., Kaser, G., Ligtenberg, S., Bolch, T., Sharp, M., Hagen, J., Van den Broeke, M., Paul, F., 2013. A reconciled estimate of glacier contributions to sea level rise: 2003 to 2009. Science (New York, N.Y.) 340, 852–857.
Huss, M., 2013. Density assumptions for converting geodetic glacier volume change to mass change. The Cryosphere 7 (3), 877–887.
Huss, M., Farinotti, D., Bauder, A., Funk, M., 2008. Modelling runoff from highly glacierized alpine drainage basins in a changing climate. Hydrol. Process. 22 (19), 3888–3902.
Huss, M., Hock, R., 2018. Global-scale hydrological response to future glacier mass loss. Nature Climate Change 8 (2), 135–140.
Immerzeel, W.W., van Beek, L.P.H., Konz, M., Shrestha, A.B., Bierkens, M.F.P., 2012. Hydrological response to climate change in a glacierized catchment in the Himalayas. Climatic Change 110 (3), 721–736.
Ismail, M.F., Naz, B.S., Wortmann, M., Disse, M., Bowling, L.C., Bogacki, W., 2020. Comparison of two model calibration approaches and their influence on future projections under climate change in the Upper Indus Basin. Climatic Change 163 (3), 1227–1246.
Jarosch, A.H., Schoof, C.G., Anslow, F.S., 2013. Restoring mass conservation to shallow ice flow models over complex terrain. The Cryosphere 7 (1), 229–240.
Jost, G., Moore, R.D., Menounos, B., Wheate, R., 2012. Quantifying the contribution of glacier runoff to streamflow in the upper Columbia River Basin. Canada. Hydrol. Earth System Sci. 16 (3), 849–860.
Kaser, G., Cogley, J.G., Dyurgerov, M.B., Meier, M.F., Ohmura, A., 2006. Mass balance of glaciers and ice caps: Consensus estimates for 1961?2004. Geophys. Res. Lett. 33 (19). _eprint: https://agupubs.onlinelibrary.wiley.com/doi/pdf/10.1029/2006GL027511.
Kay, A.L., Davies, H.N., Bell, V.A., Jones, R.G., 2009. Comparison of uncertainty sources for climate change impacts: Flood frequency in England. Climatic Change 92 (1), 41–63.
Lutz, A.F., Immerzeel, W.W., Kraaijenbrink, P.D.A., Shrestha, A.B., Bierkens, M.F.P., 2016. Climate Change Impacts on the Upper Indus Hydrology: Sources, Shifts and Extremes. PLOS ONE 11 (11), e0165630, publisher: Public Library of Science.
Maurer, E.P., Hidalgo, H.G., Das, T., Dettinger, M.D., Cayan, D.R., 2010. The utility of daily large-scale climate data in the assessment of climate change impacts on daily streamflow in california 14 (6), 1125–1138.
Meier, M.F., 1969. Glaciers and Water Supply. Journal - AWWA 61 (1), 8–12.
Meyer, J., Kohn, I., Stahl, K., Hakala, K., Seibert, J., Cannon, A.J., 2019. Effects of univariate and multivariate bias correction on hydrological impact projections in alpine catchments. Hydrol. Earth Syst. Sci. 23 (3), 1339–1354.
Moore, R., 2006. Stream Temperature Patterns in British Columbia, Canada, Based on Routine Spot Measurements. Canadian Water Resour. J. 31, 41–56.
Moore, R.D., Fleming, S.W., Menounos, B., Wheate, R., Fountain, A., Stahl, K., Holm, K., Jakob, M., 2009. Glacier change in western North America: influences on hydrology, geomorphic hazards and water quality. Hydrol. Process. 23 (1), 42–61.
Najafi, M.R., Moradkhani, H., Jung, I.W., 2011. Assessing the uncertainties of hydrologic model selection in climate change impact studies. Hydrol. Process. 25 (18), 2814–2826.
Naz, B.S., Frans, C.D., Clarke, G.K.C., Burns, P., Lettenmaier, D.P., 2014. Modeling the effect of glacier recession on streamflow response using a coupled glacio-hydrological model. Hydrol. Earth Syst. Sci. 18 (2), 787–802.
Orth, R., Staudinger, M., Seneviratne, S.I., Seibert, J., Zappa, M., 2015. Does model performance improve with complexity? A case study with three hydrological models. J. Hydrol. 523, 147–159.
Prudhomme, C., Davies, H., 2009. Assessing uncertainties in climate change impact analyses on the river flow regimes in the UK. Part 1: Baseline climate. Climatic Change 93 (1), 177–195.
Prudhomme, C., Davies, H., 2009. Assessing uncertainties in climate change impact analyses on the river flow regimes in the UK. Part 2: Future climate. Climatic Change 93 (1), 197–222.
Quick, M.C., 1995. The UBC Watershed Model. In: Computer Models in Watershed Hydrology. Water Resources Publications, Highlands Ranch, CO.
Quick, M.C., Pipes, A., 1977. U.B.C. WATERSHED MODEL. Hydrol. Sci. Bull. 22 (1), 153–161.
Radić, V., Hock, R., 2011. Regionally differentiated contribution of mountain glaciers and ice caps to future sea-level rise. Nat. Geosci. 4, 91–94.
Schiefer, E., Menounos, B., Wheate, R., 2007. Recent volume loss of British Columbian glaciers, Canada. Geophys. Res. Letters 34 (16).
Seibert, J., Vis, M.J.P., Kohn, I., Weiler, M., Stahl, K., 2018. Technical note: Representing glacier geometry changes in a semi-distributed hydrological model. Hydrol. Earth Syst. Sci. 22 (4), 2211–2224.
Simard, M., Pinto, N., Fisher, J.B., Baccini, A., 2011. Mapping forest canopy height globally with spaceborne lidar. J. Geophys. Res.: Biogeosciences 116 (G4).
Stahl, K., Moore, R.D., 2006. Influence of watershed glacier coverage on summer streamflow in British Columbia, Canada. Water Resour. Res. 42 (6).
Troin, M., Poulin, A., Baraer, M., Brissette, F., 2016. Comparing snow models under current and future climates: Uncertainties and implications for hydrological impact studies. J. Hydrol. 540, 588–602.
Tsuruta, K., Schnorbus, M.A., 2021. Exploring the operational impacts of climate change and glacier loss in the upper Columbia River Basin, Canada. Hydrol. Process. 35 (7), e14253. _eprint: https://onlinelibrary.wiley.com/doi/pdf/10.1002/hyp.14253.
van Tiel, M., Stahl, K., Freudiger, D., Seibert, J., 2020. Glacio-hydrological model calibration and evaluation. Wiley Interdisciplinary Reviews: Water 7.
Welch, B.L., 1947. The generalization of “Student’s problem when several different population varlances are involved. Biometrika 34 (1–2), 28–35.
Werner, A.T., Cannon, A.J., 2016. Hydrologic extreme—an intercomparison of multiple gridded statistical downscaling methods. Hydrol. Earth Syst. Sci. 20 (4), 1483–1508.
Werner, A.T., Schnorbus, M.A., Shrestha, R.R., Cannon, A.J., Zwiers, F.W., Dayon, G., Anslow, F., 2019. A long-term, temporally consistent, gridded daily meteorological dataset for northwestern North America. Sci. Data 6, 180299.
Zhao, J., Bose, B., 2002. Evaluation of membership functions for fuzzy logic controlled induction motor drive. In: IEEE 2002 28th Annual Conference of the Industrial Electronics Society. IECON 02. Vol. 1. pp. 229–234 vol 1.